Mutual coupling reduction of two PIFAs with a T-shape slot impedance transformer for MIMO mobile terminals

Zhang, Shuai; Lau, Buon Kiong; Tan, Yi; Ying, Zhinong; He, Sailing

Published in:
IEEE Transactions on Antennas and Propagation

DOI:
10.1109/TAP.2011.2180329

2012

Document Version:
Peer reviewed version (aka post-print)

Mutual Coupling Reduction of Two PIFAs with a T-shape Slot Impedance Transformer for MIMO Mobile Terminals

Shuai Zhang, Buon Kiong Lau, *Senior Member, IEEE,* Yi Tan, Zhinong Ying, *Senior Member, IEEE,* and Sailing He, *Senior Member, IEEE*

***Abstract*—An efficient technique is introduced to reduce mutual coupling between two closely spaced PIFAs for MIMO mobile terminals. The proposed mutual coupling reduction method is based on a T-shape slot impedance transformer and can be applied to both single-band and dual-band PIFAs. For the proposed single-band dual PIFAs, the 10 dB impedance bandwidth covers the 2.4 GHz WLAN band (2.4-2.48 GHz), and within the WLAN band an isolation of over 20 dB is achieved. Moreover, the dual-band version covers both the WLAN band and the WiMAX band of 3.4-3.6 GHz, with isolations of over 19.2 dB and 22.8 dB, respectively. The efficiency, gain and radiation patterns of the two-PIFA prototypes are verified in measurements. Due to very low pattern correlation and very good matching and isolation characteristics, the capacity performances are mainly limited by radiation efficiency. The single-band and dual-band PIFAs are also studied with respect to their locations on the ground plane. An eight-fold increase in the bandwidth of one PIFA is achieved, when the single-band PIFAs are positioned at one corner of the ground plane, with the bandwidth of the other PIFA and the good isolation unchanged.**

***Index Terms*—Antenna array mutual coupling, MIMO systems, parasitic antennas**

I. Introduction

MULTIPLE-INPUT and multiple-output (MIMO) technology has become an important feature in all future generation wireless communication systems. This is primarily because it can linearly increase channel capacity with an increase in the number of antennas, without needing additional frequency spectrum or power. Moreover, popular wireless communication systems typically operate in rich scattering environments, which MIMO exploits to achieve the aforesaid large performance gain. However, the requirement for compactness of MIMO-enabled user terminals in mobile communications can potentially induce very high mutual coupling among the antenna elements, which can dramatically degrade the MIMO systems' performance. This motivates the need for efficient isolation enhancement techniques for portable MIMO terminals [1]-[6].

Planar inverted-F antennas (PIFAs) have been widely utilized in mobile terminals due to the advantages of low profile, low cost and ease of design. However, in order to obtain an isolation of 20 dB or more between two PIFAs with air substrate on a common ground plane, their separation distance should exceed one half of the free space wavelength [7]. Even a 10 dB isolation, which is usually sufficient to achieve low enough correlation for good MIMO performance, will still require an antenna separation of a quarter of the wavelength. Moreover, this conclusion applies to three different joint orientations (co-linear, orthogonal and parallel) of the two PIFAs, which indicates limited flexibility in using different relative antenna orientations to reduce coupling. In recent years, many studies have been performed to find more efficient ways to enhance the isolation between closely-positioned PIFAs, e.g., [8]-[17]. In [8], good isolation is achieved by equipping each of the two PIFAs with a small (local) ground plane, which is physically separated from the common ground plane beneath. However, the achieved separation between the two modified PIFAs is still relatively large. Defected ground structures (DGS) can provide a band stop property and have been studied in [9]-[11]. This method can reduce the mutual coupling between antenna elements, but at the price of sacrificing impedance bandwidth and occupying too much space. A neutralization line is inserted in-between two PIFAs in [12]-[13]. This method can introduce some current on the neutralization lines and create an additional electromagnetic field to cancel the mutual coupling. Another technique, based on the former study in [12], utilizes instead a parasitic element that has no direct connection to the antenna elements to provide the decoupling field [14], [15]. Unfortunately, no matter how the neutralization line or parasitic element is positioned, they will still occupy some areas between the antennas. In [16], the quarter wavelength slot formed by the edges of two very closely positioned PIFAs is utilized to induce a resonant mode, which effectively traps the displacement (or over-the-air) coupling current between the antenna elements and enhances isolation. Hence, no additional physical structure is required by this approach. In order to further reduce mutual coupling, a new resonant mode is excited in [17], which utilizes

The work was supported in part by VINNOVA under Grant no. 2008-00970 and 2009-04047 and also in part by a scholarship within the EU Erasmus Mundus External Cooperation Window TANDEM.

S. Zhang and S. He are with the Department of Electromagnetic Engineering, School of Electrical Engineering, Royal Institute of Technology, S-100 44 Stockholm, Sweden and also with the Centre for Optical and Electromagnetic Research, Zhejiang University, Hangzhou 310058, China (e-mail: sailing@ieee.org).

B. K. Lau and Y. Tan are with the Department of Electrical and Information Technology, Lund University, SE-221 00 Lund, Sweden.

Z. Ying is with Research and Technology, Corporate Technology Office, Sony Ericsson Mobile Communications AB, SE-221 88 Lund, Sweden.

the edges of two PIFAs as well as another slot cut on the ground plane to form a half-wavelength U-shape slot in-between. Apart from trapping the displacement coupling current between the antennas, the new mode also traps the coupling current on the ground plane in the U-shape slot. Thus, the resonant mechanism of the slot effectively cuts off all coupling currents and allows an isolation of above 40dB to be realized in simulation for an inter-PIFA spacing of 0.0016 wavelength. However, the methods in [16] and [17] cannot be utilized for a ground plane with arbitrary size and shape, (e.g., that of a mobile phone), because it may not be possible to match the decoupling slots well enough in these cases in order to excite them successfully. Moreover, these methods cannot be used for dual-band applications, which further limit their versatility.

In this paper, a T-shape slot is inserted at the end of a quarter-wavelength decoupling slot formed by the edges of two PIFAs, as an impedance transformer for the decoupling slot. By appropriately adjusting the length of the T shape, the formed decoupling slot can be excited in a ground plane of arbitrary size and shape. In addition, with the help of the T-shape slot impedance transformer, a dual-band MIMO antenna with good isolation in both bands can be achieved.

The paper is organized as follows: In Section II, an impedance matching T-shape slot is introduced in a single-band two-PIFA array with a decoupling slot for mobile phone applications. Section III extends the proposed method to the dual-band case, where a dual-band isolation property can be achieved. The diversity and MIMO capacity performances of proposed single-band and dual-band antennas are evaluated in Section IV. Finally, our conclusions are presented in Section V.

II. Closely Spaced Single-Band PIFAs with a T-Shape Slot Impedance Transformer for Mobile Terminals

A. Antenna Configuration and Physical Mechanism

Figure 1 illustrates the configuration of our proposed single-band PIFAs for mobile terminals. The ground plane is a PCB with a surface area of 40 mm × 100 mm, and it consists of a 0.03 mm thick top copper sheet (i.e., the yellow region in Fig. 1) and a 1.55 mm thick FR4 substrate (i.e., the orange region in Fig. 1). The FR4 substrate has a dielectric permittivity of 4.7 and a loss tangent of 0.015. In order to simplify fabrication (i.e., a pre-requisite for mass production), the proposed PIFAs are mounted on a 1 mm thick hollow carrier (a dielectric supporting structure indicated in blue in Fig. 1) commonly found in today's terminal antenna implementations. The carrier has a dielectric permittivity and a loss tangent of 2.5 and 0.007, respectively. The two PIFAs have an edge-to-edge separation distance of 0.0088 wavelength. Each PIFA is fed by a feeding pin provided by the inner conductor of a 50Ω coaxial cable (see Figs. 1(d), 1(f) and 1(g)). In order to increase the impedance bandwidth at the end of each probe, an $L_c \times W_c$ copper sheet is added to form a capacitively load feed [18]. In this paper, the copper sheet width W_c is also an important parameters for enhancing the isolation. Since the spacing between the copper sheet and the top part of PIFA will highly affect the performance of the PIFAs, and in order to further simplify precise antenna fabrication, an $L_c \times W_c$ dielectric block is added to this in-between region. The dielectric block is of the same material as the hollow carrier and has a thickness of 1 mm. A T-shape slot is etched on the ground plane and it performs as an impedance transformer of the slot formed by the edges of two PIFAs. The detailed dimensions of the designed dual-PIFA structure are provided in Fig. 1.

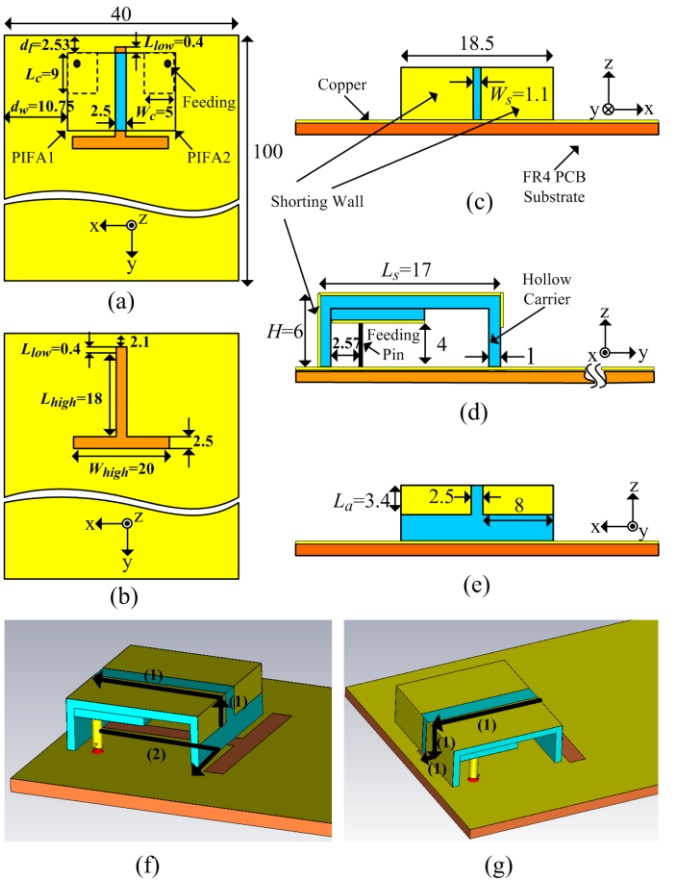

Fig. 1. Geometry of the proposed single-band PIFA array: (a) top view, (b) ground plane, (c) back view, (d) side view, (e) front view, (f) and (g) 3D view. All dimensions are given in mm.

The physical decoupling mechanism for the proposed MIMO antennas is as follows: when two PIFAs with shorting walls are positioned side-by-side, the neighboring edges of the PIFAs form a quarter-wavelength slot. For some specific sizes of the ground plane, the formed slot can be excited to reduce mutual coupling [16]. However, in general (e.g., in mobile terminals), the slot may not be able to effectively decouple the antennas. This is because different sizes of ground plane will strongly affect the impedance of the formed quarter-wavelength slot, as well as the current distributions on the ground plane, such that good matching cannot be guaranteed for the decoupling slot. To address this problem, a T-shape slot is etched on the ground plane and can be view as an impedance transformer of the formed slot. In our design, route (1) (see Figs. 1(f) and 1(g)) and route (2) (see Fig. 1(f)) are the formed decoupling slot (of length $L_a + L_s + H + L_{low}$) and the T-shape impedance transformer (of length $L_{high} + W_{high}/2$) of the formed slot, respectively. By proper optimization of the parameters L_{high} and W_{high},, the

decoupling slot formed by the edges of the PIFAs can be placed at an arbitrary location on the ground plane and efficiently excited, irrespective of the ground plane's size and shape. The simulated scattering (or S) parameters of two PIFAs with and without the T-shape impedance transformer are presented in Fig. 2. The full-wave antenna simulations are carried out in the frequency domain using the CST Microwave Studio software. It can be seen that, because of the proposed T-shape slot, the coupling between the PIFAs is reduced from -6.3 dB to less than -40 dB at the center frequency.

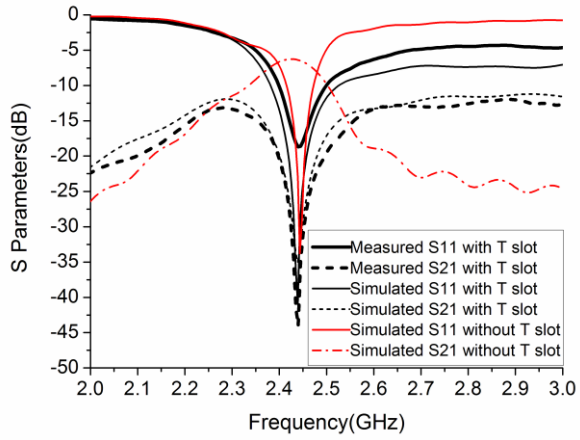

Fig. 2. Simulated S parameters with and without the T-shape slot impedance transformer, and measured S parameters of the proposed single-band PIFAs for MIMO terminals.

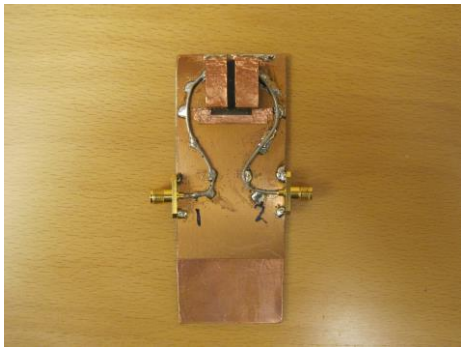

Fig. 3. Prototype of the proposed single-band PIFAs for MIMO terminals.

B. Measurement Results

The fabricated prototype of the proposed single-band PIFAs with a T-shape slot impedance transformer is presented in Fig. 3. In the mockup, two 50Ω coaxial cables are utilized, and the outer conductors of the cables are connected to the ground plane and the inner conductors are used to feed the PIFAs at the feeding pin positions shown in Fig. 1(d). The simulated and measured S parameters for the proposed PIFAs are given in Fig. 2. As can be observed, the measured results agree well with the simulated ones. The measured 10 dB impedance bandwidth is 100 MHz (2.4-2.5 GHz), which covers the WLAN band (2.4-2.48 GHz). The isolation within the 100 MHz band is over 20 dB, and up to a maximum of 44 dB.

Fig. 4 shows the measured normalized radiation gain pattern for PIFA1 (labeled in Fig. 3), which is obtained in an anechoic chamber. The measured pattern for PIFA2 is omitted here, since it is in mirror symmetry to the pattern of PIFA1. During the measurement, when PIFA1 (see Fig 1(a) or Fig. 2) is measured, PIFA2 is terminated with a 50Ω load, and vice-versa. The measured peak gain and efficiency are 1.8 dBi and 70%, respectively. The measured efficiency is obtained with an error tolerance of about 13% (0.6 dB). In addition, the loss in antenna efficiency is mainly attributed to the lack of high precision in the fabrication process (e.g., the copper tape on the carrier is cut by hand). Based on the simulation results, it can be estimated that the efficiency can be increased by 10% or more if a more professional fabrication process is applied.

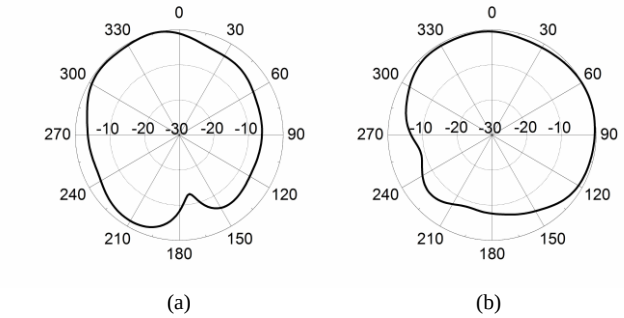

(a) (b)

Fig. 4. Measured normalized radiation gain pattern of PIFA1 at 2.45 GHz: (a) x-z plane (H-plane), (b) y-z plane (E-plane).

C. Parametric Study

To analyze the influence of different parameters and further understand the decoupling mechanism, a parametric study is performed in CST. To reduce computation time, the mesh lines per wavelength and lower mesh line limit are both set to 25, which are less than that used to obtain Fig. 2 (i.e., 45). However, this reduction is found to have only a small impact on accuracy. The results from the parametric study are summarized below:

1) Impedance matching: Figure 5 shows the influence of the capacitively loaded copper sheet of dimensions $L_c \times W_c$. It can be deduced that L_c and W_c mainly determine the impedance matching of the PIFAs. Furthermore, when W_c increases, the mutual coupling will also increase (see Fig. 5(b), where at 2.35 GHz, W_c = 7 mm has a worse impedance matching and a stronger coupling than W_c = 5 mm). Moreover, we found that the effects of changing L_c are similar to those of changing W_c, though not as significant.

2) Matching of decoupling slot: In order to enhance the isolation between the PIFAs, the formed decoupling slot should be well matched. As shown in Fig. 6, the matching characteristic is mainly determined by the size of the T-shape slot (L_{high}, W_{high}) on the ground plane. It can be observed that mutual coupling can be effectively reduced by a properly dimensioned T-shape slot. Figure 6 also reveals that the T-shape slot has little impact on the operating frequency and the coupling null, and this indicates that it is not a part of the PIFAs' radiating structure.

3) Location of coupling null: In Fig. 7, the influence of the parameters W_s and L_{low} are presented. When W_s is progressively increased, the coupling null moves to a higher frequency at a faster rate than the operating frequency. On the other hand, an

increase in L_{low} will result in the coupling null moving to a lower frequency at a faster rate than the operating frequency. By optimizing W_s or L_{low}, the operating frequency and coupling null can be made to coincide, whereas the isolation level can be tuned by adjusting the dimensions of the T-shape slot.

D. Current Distributions

The current distribution of the proposed single-band PIFAs is shown in Fig. 8. This distribution is obtained when PIFA1 is excited. It can be observed that: First, most of the coupling current is trapped in the formed slot and cannot flow to PIFA2, and thus good isolation is achieved by the two PIFAs. Second, the current distribution along route (1) (see Figs. 1(g) and 1(f)) is similar to that of a conventional quarter-wavelength slot, where the current is very strong at the feeding end (i.e., observe the current distribution at the L_{low} part in Figs.1(a) and 1(b)). In contrast, the current along route (2) of length $L_{high}+W_{high}/2$ (see Fig. 1(g)) is significantly weaker, because it only works as a T-shape impedance transformer of the decoupling slot and contributes very little to the antenna radiation.

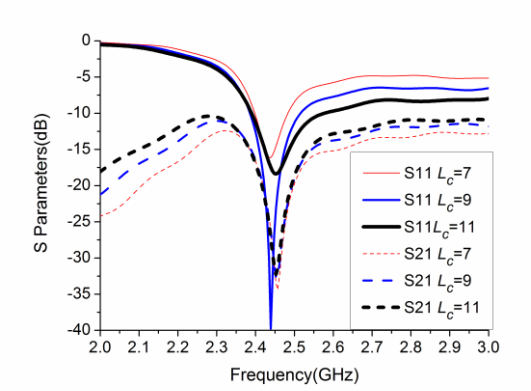

(a)

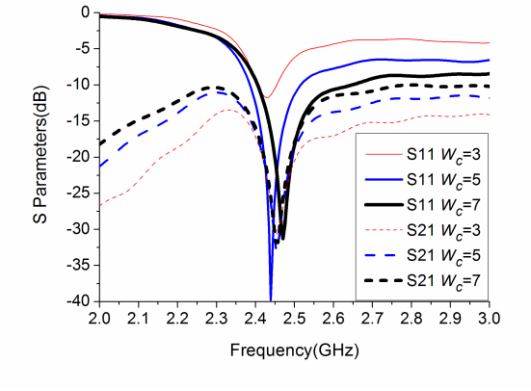

(b)

Fig. 5. Impact of the capacitively loaded copper sheet parameters: (a) length L_c, (b) width W_c.

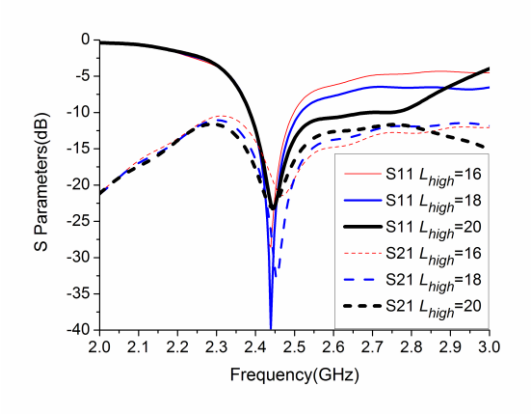

(a)

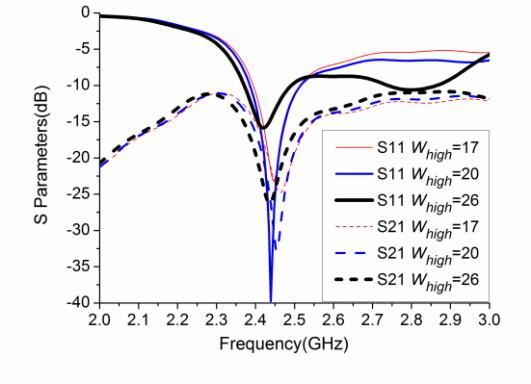

(b)

Fig. 6. Impact of the T-shape slot parameters: (a) length L_{high}, (b) width W_{high}.

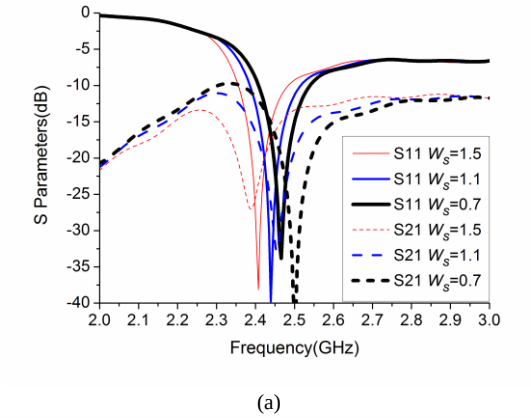

(a)

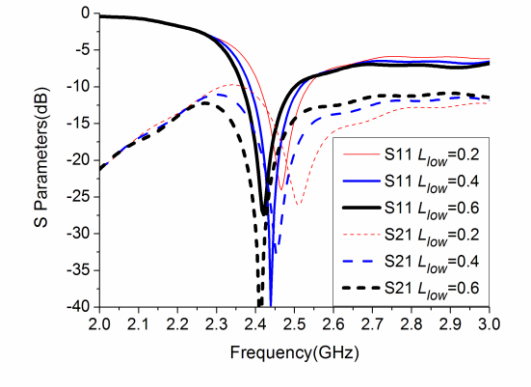

(b)

Fig. 7. Impact of the decoupling slot parameters: (a) W_s, (b) L_{low}.

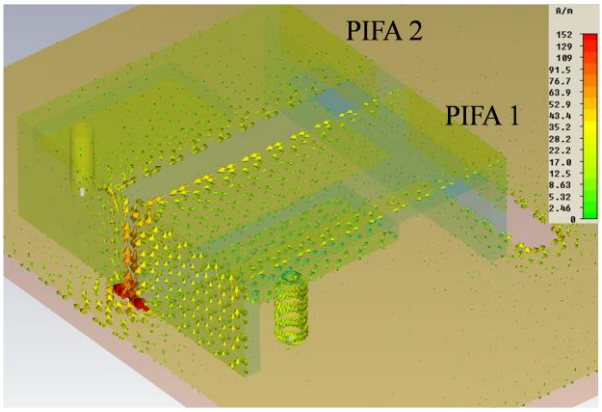

Fig. 8. Current distribution of the proposed single-band PIFAs for MIMO terminals at 2.45 GHz.

E. Study of the Dual-PIFA Location

To demonstrate the versatility of the proposed dual-PIFA structure in terms of its location on the ground plane, it is moved from the upper center position (see Fig. 1) to the upper left corner of the ground plane, as illustrated in Fig. 9. The detailed parameters of the PIFAs at this new location are given in Table I, though only the parameters that are changed, relative to those of the previous location, are listed. This new case reveals that our proposed method can also work for an asymmetrical structure. The simulated S parameters are presented in Fig. 10. It is observed that the impedance bandwidth for PIFA1 has been significantly enlarged. PIFA1 and PIFA2 can cover the bands of 2.3-3.1 GHz and 2.4-2.5 GHz (WLAN band), respectively (for the -10 dB specification). Within the WLAN band where MIMO can be applied (since it is covered by both PIFAs), the isolation between PIFA1 and PIFA2 is at 15 dB. Moreover, the isolation is above 11 dB over the full bandwidth of PIFA1, suggesting that the additional bandwidth (outside the WLAN band) may be good enough for other wireless applications.

The mechanisms for the much larger bandwidth of PIFA1 are explained as follows: First, when the PIFA array moves from the upper center location to the upper left corner location, another resonant mode is introduced by the T-shape slot. In this case, the T-shape slot works not only as an impedance transformer for the decoupling slot (at 2.45 GHz), but also as one part of PIFA1 to provide another resonance (at around 2.9 GHz). This is the main reason for the larger bandwidth of PIFA1. Second, it is much easier for a PIFA (PIFA1 in this case) to excite the so-called chassis mode, when its longer side is placed along the edge of the ground plane [19]-[22], and this mode can further increase the bandwidth. Based on these two mechanisms, the impedance bandwidth of PIFA1 can be efficiently enlarged by eight times. Moreover, the 15 dB isolation within the WLAN band can be further enhanced, if the size of the T-shape slot increases. However, an improved isolation can only be achieved at the cost of a smaller PIFA1 bandwidth. This is because the T-shape slot provides the higher resonant frequency for the bandwidth of PIFA1, and when it is enlarged, the resonance will move to a low frequency.

TABLE I
CHANGED PARAMETERS OF THE PIFAS AT THE CORNER OF THE GROUND PLANE

Parameters	d_w	d_l	L_{low}	$L_c^{(1)}$	$L_c^{(2)}$	$W_c^{(1)}$	$W_c^{(2)}$
Value(mm)	2.75	0.5	0.2	15	8	5	5
Parameters	$La^{(1)}$	$La^{(2)}$	W_s				
Value(mm)	3	3.1	0.5				

N.B. $^{(1)}$,$^{(2)}$ represent the changed parameters for PIFA1 and PIFA2, respectively.

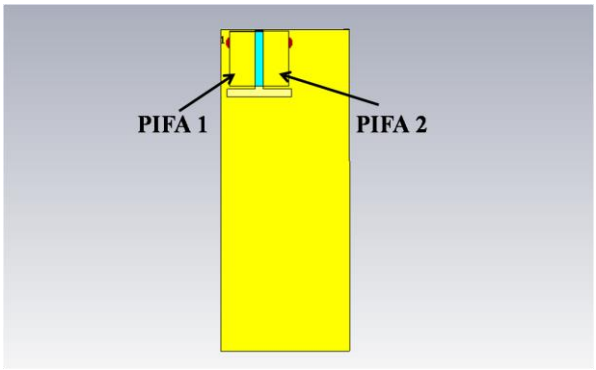

Fig. 9. Schematic drawing of the single-band PIFAs at the corner location.

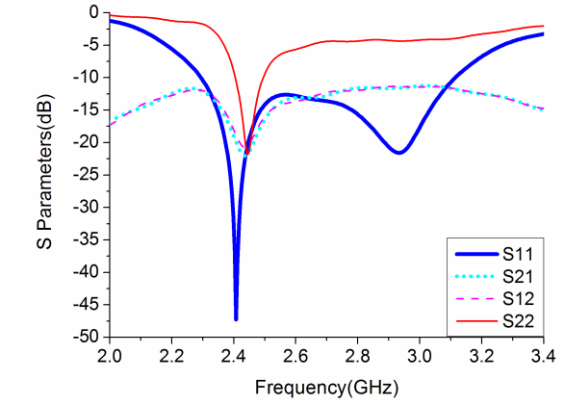

Fig. 10. S parameters of the single-band PIFAs at the corner location.

Furthermore, when the PIFA array is rotated by 90° and place on one corner of the ground plane, the results are very similar to the case studied before. The PIFA close to the shorter edge of the ground plane will have a much larger bandwidth and for the other one the bandwidth remains almost the same. The trade-off between the isolation of the two PIFAs and the bandwidth of the PIFA closer to the short edge also exists.

III. CLOSELY SPACED DUAL-BAND PIFAS WITH A T-SHAPE SLOT IMPEDANCE TRANSFORMER FOR MIMO TERMINALS

A. Antenna Geometry and Physical Mechanism

The proposed decoupling method can also be extended to dual-band MIMO applications. The configurations for the designed dual-band PIFAs are shown Fig. 11. The materials used in this designed are the same as those of the single-band case. Each PIFA is fed by a feeding pin provided by the inner conductor of a 50Ω coaxial cable (see Figs. 11(d), 11(f) and 11(g)). At the end of each probe, an $L_c \times W_c$ copper sheet is added and directly pasted onto the inner surface of the hollow

carrier. Different from the single-band case, a folded L-shape slot (see route (3) in Fig. 11 (a)) is etched onto each PIFA and some metal parts are removed in Fig. 11(e) (as compared to Fig. 1(e)) to change the length of the L slot. By optimizing all parameters properly, a dual-band dual-isolation property can be achieved, as shown in Fig. 12.

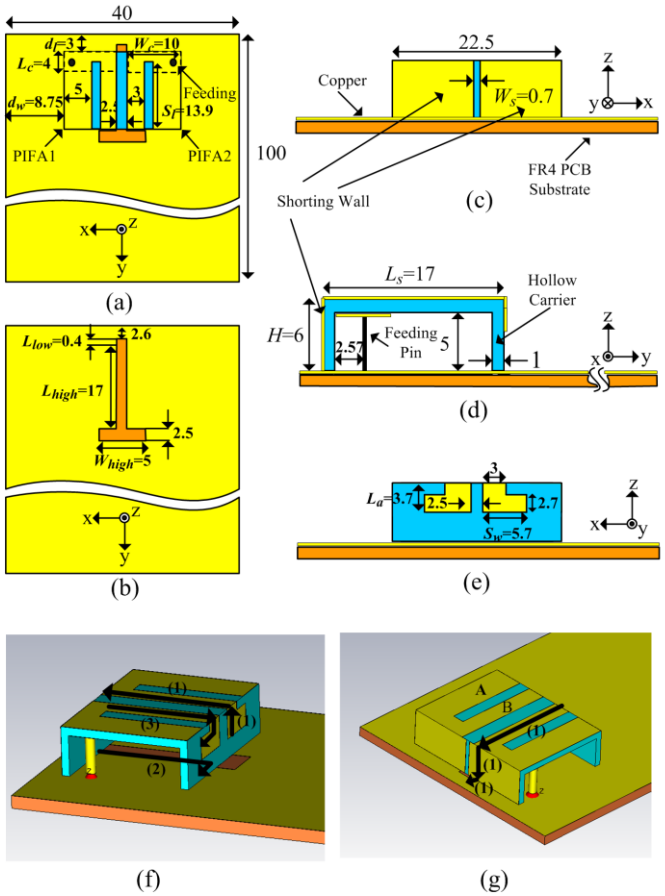

Fig.11. Geometry of the proposed dual-band PIFA array: (a) top view, (b) ground plane, (c) back view, (d) side view, (e) front view, (f) and (g) 3D view. All dimensions are given in mm.

The physical mechanism for the dual-band dual-isolation property of the proposed MIMO antennas is described as follows: For the WLAN band (2.4-2.48 GHz), the decoupling mechanism is the same as the single-band case and has been explained in Section II-A. Regarding the 3.5 GHz band, the operating bandwidth can be determined by part "A" (see Fig. 11(g)) and the decoupling property is achieved by the folded L slot (see route (3) in Fig. 11(f)) formed by parts "A" and "B" in Fig. 11(g). Similar to the case of the WLAN band, the formed decoupling L slot also needs to be matched well to work correctly, and the T-shape slot can also tune the impedance matching of the L slot. In the dual-band case, the T-shape slot is mainly responsible for the matching of the decoupling L slot. However, this will result in a slight mismatch of the decoupling slot formed by the two PIFAs in the WLAN band. In order to solve this problem, another parameter W_c is utilized together with the T-shape slot to adjust the matching of the formed decoupling slot in the WLAN band. Therefore, a dual-band dual-isolation property can be achieved. The simulated S parameters between two PIFAs with and without T-shape impedance transformer are show in Fig. 12. It can be seen that the isolation is significantly enhanced with the T-shape slot.

B. Measurement Results

The fabricated prototype of the proposed dual-band PIFAs for MIMO terminals is shown in Fig. 13. In the fabricated mockup, the feeding method is the same as that of the single-band case. A comparison between the measured and simulated S parameters can be obtained from Fig. 12. Based on the measured results, the proposed dual-band MIMO antennas can cover the 2.4-2.48 GHz WLAN band and the 3.4-3.6 GHz WiMAX band (for the -10 dB specification). Within the operating band, the isolations are above 19.2 dB at the lower band and above 22.8 dB at the higher band. In general, the measured and simulated results agree well with each other. Although there is a slight difference between simulation and measurement in the frequency of the coupling null at the higher band, the worst isolation (22.8 dB) within the operating band is still above 20 dB.

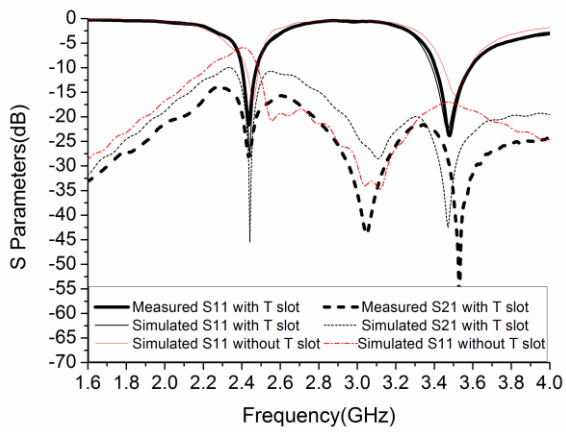

Fig. 12. Simulated S parameters with and without the T-shape slot impedance transformer, and measured S parameters of the proposed dual-band PIFAs for MIMO terminals.

Fig. 13. Prototype of the proposed dual-band PIFAs for MIMO terminals.

The measured normalized radiation gain patterns of PIFA1 at 2.44 GHz and 3.5 GHz are presented in Fig. 14. The peak gain and efficiency are also measured. As before, the error tolerance of the efficiency measurement is about 13% (0.6 dB). In the WLAN band and the WiMAX band, the peak efficiencies

are 70.3% and 77.2%, respectively, whereas the peak gains are 2.4 dB and 3.4 dB, respectively. These efficiencies and gains are good enough for MIMO terminal applications.

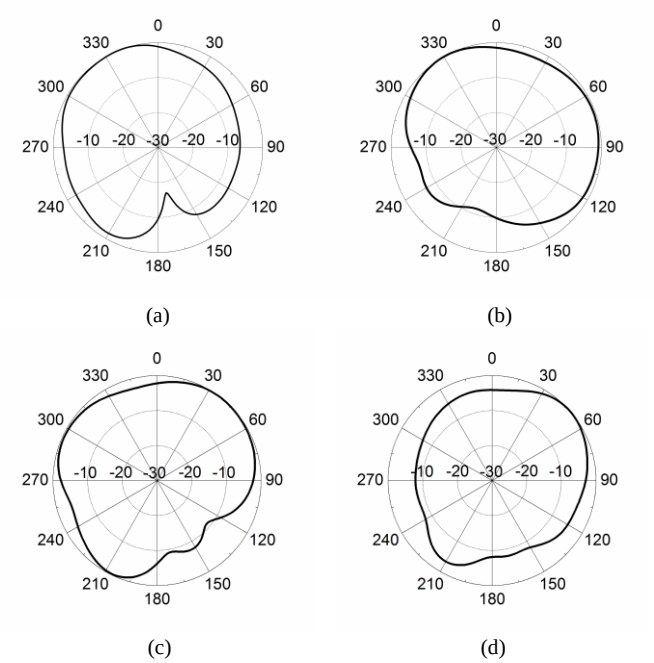

Fig. 14. Measured normalized radiation gain patterns of PIFA1: (a) x-z plane (H-plane) at 2.44 GHz, (b) y-z plane (E-plane) at 2.44 GHz, (c) x-z plane (H-plane) at 3.5 GHz, (d) y-z plane (E-plane) at 3.5 GHz.

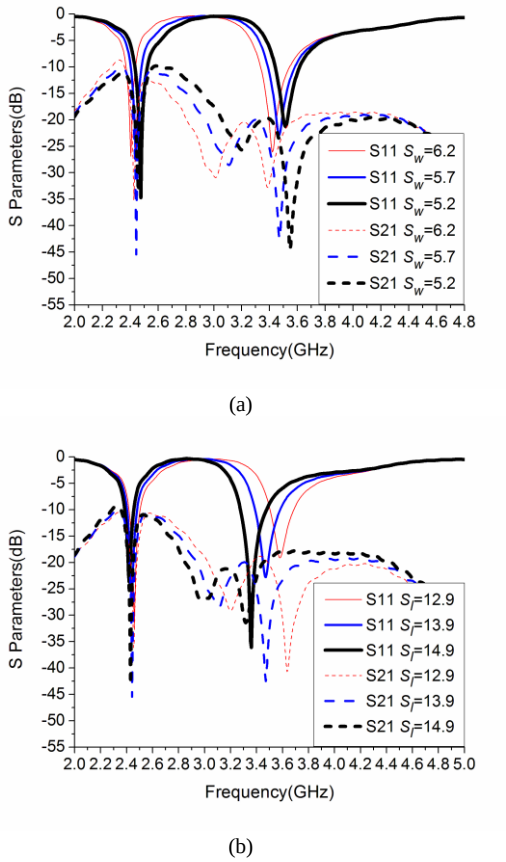

Fig. 15. Impact of parameters (a) S_w, (b) S_l.

C. *Parametric Study*

In the CST simulations, to guarantee good accuracy, both the mesh lines per wavelength and lower mesh limit are set to 45.

1) S_w and S_l: The influence of the parameter S_w, which determines the length of the L decoupling slot on the PIFAs, is shown in Fig. 15(a). As the length of S_w decreases, the L decoupling slot becomes shorter, while part "A" that determines the operating frequency at the WiMAX band is unchanged (see Fig. 11(g)). As expected, the shorter decoupling slot leads to the WiMAX band coupling null moving higher in frequency. The effect of the parameter S_l can be seen in Fig. 15(b). Since a change in S_l will simultaneously increase or decrease the length of the L slot and part "A", the relative location of the coupling null and operating frequency does not change significantly over the investigated range of S_l.

2) L_c and W_c: The influences of L_c and W_c have been studied in Section II-C for the single-band case. However, apart from the aforementioned effects, they also have some new roles in the dual-band case. As illustrated in Fig. 16, L_c and W_c can affect the matching of the operating frequencies of both bands. Moreover, W_c can also change the location of the coupling null for the WiMAX band and the matching performance of the decoupling slot formed by the two PIFAs in the WLAN band. This is because the coupling current distribution can be viewed as the source or feed of the decoupling element (L slot or slot formed by two PIFAs). When the feeding condition is changed, the operating property (e.g., location of coupling null and matching performance) is also affected.

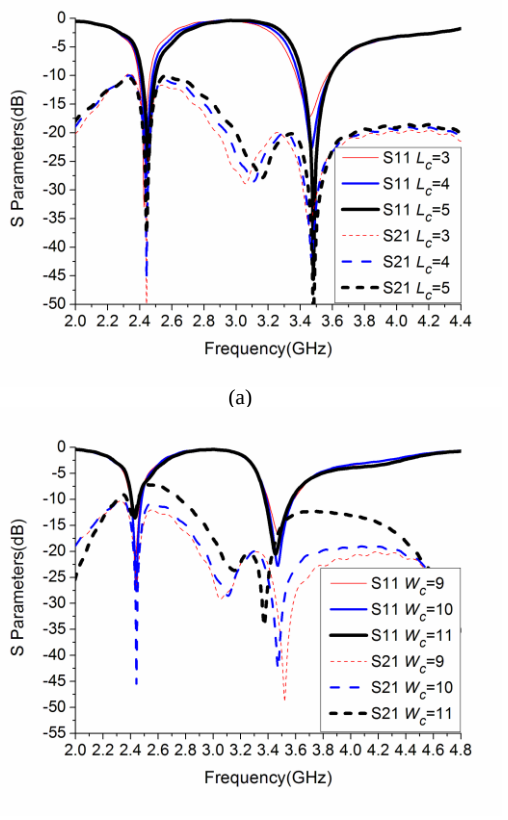

Fig. 16. Impact of the capacitively loaded copper sheet dimensions: (a) length L_c, (b) width W_c.

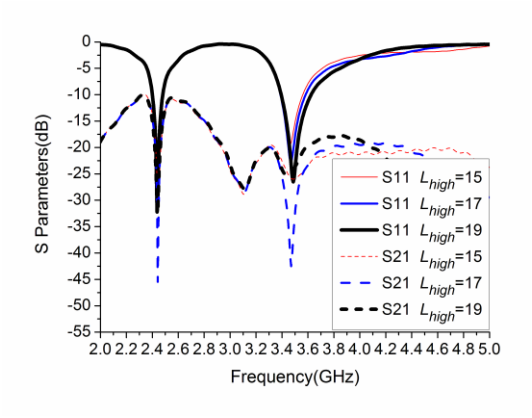

(a)

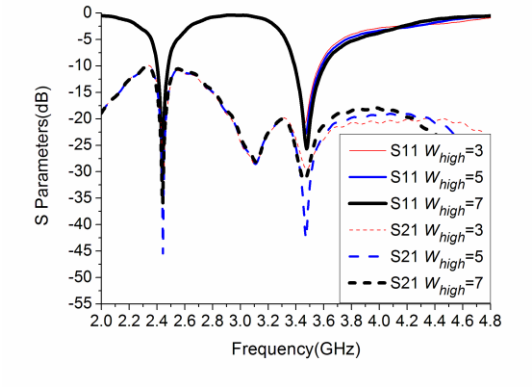

(b)

Fig. 17. Impact of the T-shape slot parameters: (a) length L_{high}, (b) width W_{high}.

3) L_{high} and W_{high}: As mentioned in the single-band case, L_{high} and W_{high} will affect the matching performance of the decoupling slot formed by the two PIFAs in the WLAN band. Nonetheless, the T-shape slot impedance transformer will likewise affect the matching performance of the decoupling L slots. In the dual-band case, these two parameters are mainly responsible for the matching performance of the decoupling L slot for the WiMAX band. For the WLAN band, they work together with W_c to tune the matching performance of the decoupling slot formed by the two PIFAs. In this way, a dual-band dual-isolation property is achieved. The influences of the T-shape slot dimensions L_{high} and W_{high} are presented in Fig. 17. Similar to the single-band case, W_s and L_{low} are mainly used to tune the location of the coupling null for WLAN band.

D. Current Distributions

The current distributions of the proposed dual-band PIFAs are given in Fig. 18 for 2.44 GHz and 3.5 GHz, which are the center frequencies of the two operating bands. At 2.44 GHz (the WLAN band), the currents are mainly concentrated on part "B" (see Figs. 11(g) and 18(a)), which determines the operating frequency of the lower band. In addition, most of the coupling currents are trapped in the slot formed by two PIFAs. At 3.5 GHz (the WiMAX band), the currents mainly focus on part "A" (see Figs. 11(g) and 18(b)) which controls the operating frequency of the higher band. The coupling currents are blocked by the L slot and thus cannot flow into the adjacent PIFA.

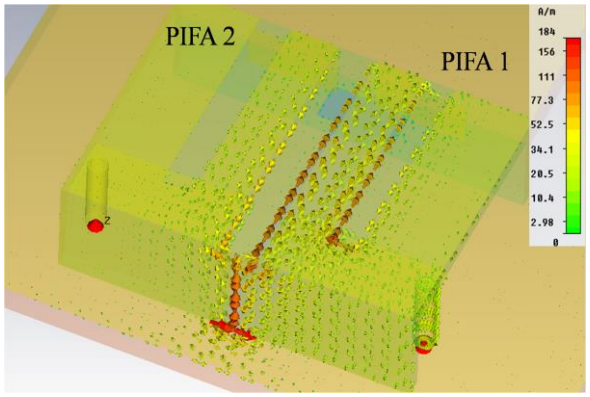

(a)

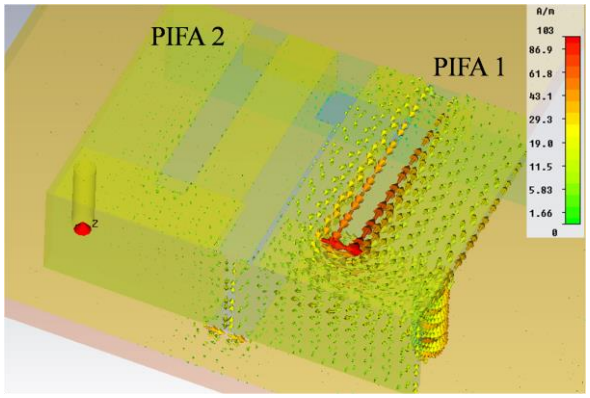

(b)

Fig. 18. Current distributions of the proposed dual-band PIFAs for MIMO terminals at (a) 2.44 GHz, (b) 3.5 GHz.

E. Study of the Dual-PIFA Location

As in the single-band case, the impact of the dual-PIFA location on the ground plane (adjusted by the parameter d_w in Fig. 11(a)) is studied for the dual-band case. For conciseness, we do not show the S parameter results of this case. Unlike the single-band case, the moving of the MIMO dual-band antennas from the center location to the corner location does not produce the wideband behavior for the antenna closer to the longer edge of the ground plane, or PIFA1 (see Fig. 10). Instead, it only offers slightly bigger bandwidths in both bands, whereas those for the other antenna (PIFA2) are slightly reduced. In addition, the coupling behavior is largely unchanged. The relatively small change in the bandwidths of PIFA1 in the dual-band case is because the parameter W_{high} of the T-shape slot is much shorter than that of the single-band case. Consequently, the T slot mode is not efficiently excited so as to enlarge the bandwidth. On the other hand, if desired, the now slightly different bandwidths of PIFA1 and PIFA2 for the corner placement can be equalized by enlarging the width of PIFA2 while reducing the width of PIFA1 (to maintain the volume of the entire PIFA array). Furthermore, the same conclusions as above apply to the case where the PIFA array at the corner location is rotated by 90°.

IV. Correlation and MIMO Channel Capacity

A. Correlation

Correlation coefficient is an important MIMO performance

metric, as it quantifies the ability of the MIMO channel to provide parallel sub-channels, which facilitates good capacity performance. The envelope correlation is defined in [23]. The envelope correlation for the proposed single-band (see Fig. 1) and dual-band (see Fig. 11) PIFA arrays are calculated with the measured 3D electric field radiation patterns by assuming uniform 3D angular power spectrum (APS). The envelope correlation coefficient for the single-band PIFA array is less than 0.09 in the band of 2.4-2.5 GHz, and for the dual-band MIMO array, the coefficients are 0.04 and 0.093 in the bands of 2.4-2.48 GHz and 3.4-3.6 GHz, respectively.

B. MIMO Channel Capacity

With the same number of transmitting and receiving antennas (i.e., 2) and without channel knowledge at the transmitter, the ergodic capacity of the 2 × 2 MIMO channel **H** in uniform 3D APS can be obtained using the measured antenna efficiencies and the complex correlation coefficient ρ_c, assuming that the PIFA array is on the receive side, and there is no correlation or coupling on the transmit side [24]

$$\overline{C} = \mathrm{E}\left\{\log_2\left[\det\left(\mathbf{I}_2 + \frac{P}{2\sigma_n^2}\mathbf{H}\mathbf{H}^H\right)\right]\right\} \quad (1)$$

where $\det(\bullet)$, $(\bullet)^H$ and $\mathrm{E}(\bullet)$ are the determinant, conjugate-transpose and expectation operators, respectively. P is the total power that is equally distributed to each transmitting antenna, σ_n^2 is the receiver noise power, $\mathbf{I}_2$ is the 2 × 2 identity matrix. Moreover, $\mathbf{H} = \mathbf{R}^{1/2}\mathbf{H}_w$, $\mathbf{R} = \mathbf{\Lambda}^{1/2}\overline{\mathbf{R}}\mathbf{\Lambda}^{1/2}$, $\mathbf{\Lambda} = \mathrm{diag}(\eta_1, \eta_2)$, where $\mathbf{H}_w$ is a 2 × 2 matrix of independent and identical distributed (i.i.d.) complex Gaussian variables with zero mean and unit variance, $\overline{\mathbf{R}}$ is a normalized correlation matrix whose diagonal elements are 1 and the upper and lower off-diagonal elements are given by ρ_c and ρ_c^*, respectively, and η_m is the total efficiency of antenna m [24], [25].

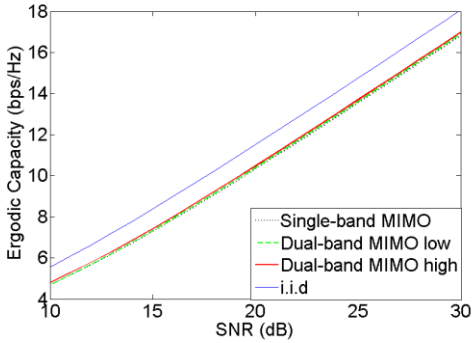

Fig. 19. Ergodic capacity for: singe-band PIFA array, dual-band PIFA array at the lower band and dual-band PIFA array at the higher band.

The ergodic capacities of the single-band and dual-band PIFA arrays are shown in Fig. 19. The reference i.i.d. Rayleigh case, i.e., with $\mathbf{R} = \mathbf{I}_2$ and $\mathbf{H} = \mathbf{H}_w$ in (1), is also shown for comparison. The results confirm that the designed PIFA arrays give good MIMO performance. The differences in SNR requirement between the i.i.d. Rayleigh case and the proposed antennas in achieving a given ergodic capacity is mainly due to reduced total efficiency, since the correlation is very low.

V. Conclusions

This paper demonstrates an efficient decoupling technique for two PIFAs that is enabled by a T-shape slot impedance transformer. The technique is not only applicable to single-band PIFAs, but also to dual-band PIFAs through a dual-isolation property. The impact of the PIFA array location on the antenna performance is studied for both single-band and dual-band cases. When the single-band PIFA array is positioned at one corner of the ground plane, the bandwidth of one PIFA can be enlarged by eight times, whereas the bandwidth of the other PIFA and the good isolation remain almost the same. Correlation and channel capacity results confirm that the proposed PIFA array can give good MIMO performance. Overall, our results substantiate that the proposed technique is both effective and versatile for practical implementation in MIMO terminals.

Finally, it is noted that the proposed technique can be applied to MIMO antennas operating in a lower frequency band, e.g., at 1.5 GHz in LTE band 21. In particular, the T-shape slot can be modified into a meander-shape slot or a slot of some other shapes to keep the whole antenna structure compact.

Acknowledgment

The authors thank Dr. Anders Sunesson of Lite-on Mobile AB, Sweden, for his help with antenna pattern measurements.

References

[1] B. K. Lau, "Multiple antenna terminals," in *MIMO: From Theory to Implementation*, C. Oestges, A. Sibille, and A. Zanella, Eds. San Diego: Academic Press, 2011, pp. 267-298.

[2] S. Zhang, Z. Ying, J. Xiong, and S. He, "Ultrawideband MIMO/diversity antennas with a tree-like structure to enhance wideband isolation," *IEEE Antennas Wireless Propag. Lett.* vol. 8, pp.1279-1282, Dec. 2009.

[3] J. Zhu and G. V. Eleftheriades, "A simple approach for reducing mutual coupling in two closely spaced metamaterial-inspired monopole antennas," *IEEE Antennas Wireless Propag. Lett.*, vol. 9, pp. 379-382, 2010.

[4] S. Zhang, P. Zetterberg, and S. He, "Printed MIMO antenna system of four closely-spaced elements with large bandwidth and high isolation," *Electron. Lett.*, vol.46, No.15, pp.1052-1053, 2010

[5] R. Tian, V. Plicanic, B. K. Lau and Z. Ying, "A compact six-port dielectric resonator antenna array: MIMO channel measurements and performance analysis," *IEEE Trans. Antennas Propag.*, vol. 58, no. 4, pp. 1369–1379, Apr. 2010.

[6] Y. J. Sung, M. Kim, and Y. S. Kim, "Harmonics reduction with defected ground structure for a microstrip patch antenna," *IEEE Antennas Wireless Propag. Lett.*, vol. 2, pp. 111–113, 2003.

[7] H. Carrasco, H. D. Hristov, R. Feick, and D. Cofre, "Mutual coupling between planar inverted-F antennas," *Microwave Opt. Technol. Lett.*, vol. 42, no. 3, pp. 224–227, Aug. 2004.

[8] Y. Gao, X. D. Chen, Z. Ying, and S. He, "Design and performance investigation of a dual-element PIFA array at 2.5 GHz for MIMO terminal," *IEEE Trans. Antennas Propag.*, vol. 55, no. 12, pp. 3433–3441, Dec. 2007.

[9] D. Ahn, J. S. Park, C. S. Kim, J. Kim, Y. Qian, and T. Itoh, "A design of the low-pass filter using the novel microstrip defected ground structure," *IEEE Microw. Theory Tech.*, vol. 49, no. 1, pp. 86–93, Jan. 2001.

[10] C. Caloz, H. Okabe, T. Iwai, and T. Itoh, "A simple and accurate model for microstrip structures with slotted ground plane," *IEEE Microwave Wireless Comp. Lett.*, vol. 14, no.4, pp. 133–135, Apr. 2004.

[11] C.-Y. Chiu, C.-H. Cheng, R. D. Murch, and C. R. Rowell, "Reduction of mutual coupling between closely-packed antenna elements," *IEEE Trans. Antennas Propag.*, vol. 55, no. 6, pp. 1732–1738, Jun. 2007.

[12] A. Diallo, C. Luxey, P. L. Thuc, R. Staraj, and G. Kossiavas, "Study and reduction of the mutual coupling between two mobile phone PIFAs

operating in the DCS1800 and UMTS bands," *IEEE Trans. Antennas Propag.*, vol. 54, no. 11, pp. 3063-3074, Nov. 2006.

[13] C. Yang, J. Kim, H. Kim, J. Wee, B. Kim, and C. Jung, "Quad-band antenna with high isolation MIMO and broadband SCS for broadcasting and telecommunication services," *IEEE Antennas Wireless Propag. Lett.*, vol. 9, pp. 584-587, 2010.

[14] A. C. K. Mak, C. R. Rowell, and R. D. Murch, "Isolation enhancement between two closely packed antennas," *IEEE Trans. Antennas Propag.*, vol. 56, no. 11, pp. 3411–3419, Nov. 2008.

[15] B. K. Lau and J. B. Andersen, "Simple and efficient decoupling of compact arrays with parasitic scatterers," *IEEE Trans. Antennas Propagat*., in press.

[16] S. Zhang, J. Xiong, and S. He, "MIMO antenna system of two closely-positioned PIFAs with high isolation," *Electon. Lett.*, vol.45, no.15, pp. 771-773, 2009.

[17] S. Zhang, S. N. Khan, and S. He. "Reducing mutual coupling for an extremely closely-packed tunable dual-element PIFA array through a resonant slot antenna formed in-between," *IEEE Trans. Antenna Propag.* vol. 58, No. 8, pp. 2771-2776, Aug. 2010.

[18] C. R. Rowell and R. D. Murch, "A capacitively loaded PIFA for compact mobile telephone handsets," *IEEE Trans. Antennas Propag.*, vol. 45, no. 5, pp. 837–842, May. 1997.

[19] J. Villanen, J. Ollikainen, O. Kivekas, and P. Vainikainen, "Coupling element based mobile terminal antenna structure," *IEEE Trans. Antennas Propagat.*, vol. 54, no. 7, pp. 2142-2153, Jul. 2006.

[20] W. L. Schroeder, A. A. Vila, and C. Thome, "Extremely small wideband mobile phone antenna by inductive chassis mode coupling," *in Proc. 36th Europ. Microw. Conf.*, Manchester, 2006, pp. 1702-1705.

[21] W. L. Schroeder and C. T. Famdie, "Utilization and tuning of the chassis modes of a handheld terminal for the design of multiband radiation characteristics," *in Proc. IEE Wideband Multiband Antennas and Arrays*, Sep. 7, 2005, pp.117-122.

[22] S. R. Best, "The significance of ground-plane size and antenna location in establishing the performance of ground-plane-dependent antennas," *IEEE Antennas Propagat. Mag.* vol. 51, no. 6, pp. 29-42, Dec. 2009.

[23] M. B. Knudsen and G. F. Pedersen, "Spherical outdoor to indoor power spectrum model at the mobile terminal," *IEEE J. Sel. Areas Commun.*, vol. 20, no. 6, pp. 1156–1168, Aug. 2002.

[24] R. Tian, B. K. Lau and Z. Ying, "Multiplexing efficiency of MIMO antennas," *IEEE Antennas Wireless Propag. Lett.*, vol. 10, pp. 183-186, 2011.

[25] J. W. Wallace and M. A. Jensen, "Modeling the indoor MIMO wireless channel," *IEEE Trans. Antennas Propag.*, vol. 50, no. 5, pp. 591-599, May 2002.